- **Exploring Trisubstituted Adenine Derivatives as Adenosine A1 Receptor**
- 2 Ligands with Antagonist Activity: Synthesis, Biological Evaluation and
- 3 Molecular Modelling
- 4 Laura B. Córdoba-Gómeza, Álvaro Lorente-Macíasb,c, María Isabel Lozad, José Bread, Antón
- 5 Leandro Martínez<sup>d</sup>, , Jonathon Mok<sup>b,c</sup>, Ben King<sup>b,c</sup>, Francisco Franco-Montalban<sup>a</sup>, Antonio
- 6 González Garcíaª, Juan José Guardia-Monteagudo¹, Maria J. Matosº\*, , Asier Unciti-Brocetab.c,
- Juan José Díaz-Mochón<sup>a,f,g,h\*</sup>, María José Pineda de las Infantas<sup>a\*</sup>
- 8 aDepartamento Química Farmacéutica y Orgánica, Facultad de Farmacia, Universidad de
- 9 Granada, Spain
- 10 bEdinburgh Cancer Research, Institute of Genetics and Cancer, The University of Edinburgh,
- 11 Crewe Road South, Edinburgh EH4 2XU, UK
- 12 °Cancer Research UK Scotland Centre, UK
- d Departamento de Farmacología, Farmacia y Tecnología Farmacéutica, Facultad de Farmacia,
- 14 CIMUS Research Center, Santiago de Compostela, Spain
- 15 °Departamento de Química Orgánica, Facultad de Farmacia, Universidade de Santiago de
- 16 Compostela, 15782 Santiago de Compostela, Spain
- <sup>f</sup>GENYO Centre for Genomics and Oncological Research, Pfizer/University of
- 18 Granada/Andalusian Regional Government. PTS Granada Avenida de la Ilustración, 114,
- 19 18016, Granada, Spain
- 20 gUnit of Excellence in Chemistry Applied to Biomedicine and the Environment of the University of
- 21 Granada, Granada, Spain
- <sup>h</sup>Instituto de Investigación Biosanitaria ibs.GRANADA, Granada, Spain
- <sup>1</sup>DESTINA Genomica SL, Avenida de la Innovación 1, 18016 Granada, Spain.
- 25 Correspondence:

- 26 Maria Joao Matos, Departamento de Química Orgánica, Facultad de Farmacia, Universidade de
- 27 Santiago de Compostela, 15782 Santiago de Compostela, Spain. mariajoao.correiapinto@usc.es

- Juan Jose Diaz-Mochon, Campus Cartuja s/n, 18071 Granada, Facultad de Farmacia,
- 29 Universidad de Granada, Spain. juandiaz@go.ugr.es
- 30 Maria Jose Pineda de las Infantas, Campus Cartuja s/n, 18071 Granada, Facultad de Farmacia
- 31 Universidad de Granada, Spain. mjpineda@ugr.es

33

34

35 important as our understanding of the physio-pathological functions of ARs advances. This study 36 presents the synthesis and biological screening of a novel library of trisubstituted adenine 37 analogues and reports the discovery of derivatives that displaying selective binding affinity 38 towards hA1AR. Compounds were synthesized using a cyclization approach by combining 4,6-39 bisalkylamino-5-aminopyrimidines with three different trialkyl/arylorthoesters, thereby generating 40 adenines featuring three different substituents at the C-8 position: H, methyl or phenyl. Most 41 promising derivatives presented a phenyl ring at such position and displayed selective antagonistic activity against hA1AR. N,9-diisopropyl-8-phenyl-9H-purin-6-amine (14c) was 42 43 identified as the most potent compound with a K of 2 nM, motivating the synthesis of new 44 derivatives including 19c. Docking modelling predicted key interactions between the lead

**Abstract:** The therapeutic potential of adenosine receptor (AR) ligands is becoming increasingly

48

49

50

51

52

53

54

47

45

46

**Keywords:** Adenine scaffold, docking simulation, cancer cell lines, antiproliferation, orthosteric binding site, selectivity index, pharmacokinetic properties

compounds and hA<sub>1</sub>AR. Determination of their anti-proliferative activity on six cancer cell lines

further exploration around the adenine scaffold for cancer research and AR drug development.

found **19c** to be the most potent derivative with low micromolar  $EC_{50}$  values. Our findings support

#### 1. Introduction

One of the most ubiquitous receptors in human cell membranes is the adenosine receptor (AR). It is a purinergic G protein-coupled receptor (GPCR) and is widely distributed in many tissues with adenosine as its endogenous agonist. There are four different types of ARs:

A<sub>1</sub>, A<sub>2A</sub>, A<sub>2B</sub> and A<sub>3</sub>, each with a variety of functions. Purines are privileged structures because they are one of the most widely occurring heterocycles in nature.<sup>1</sup> They have a low cost, commercial availability, and a range of well-established synthetic protocols existing in the literature. Additionally, purines have potential pharmacological properties that make them attractive for use in drug discovery. Furthermore, their structure allows for the generation of new purine analogues through a range of different reactions, making them an efficient chemical "navigator" towards novel compounds with desired biological activities.<sup>2</sup> To date, dozens of purine-based drugs have been approved by regulatory agencies, including fludarabine, tecadenoson, cladribine and regrelor.<sup>3</sup> Despite purines being privileged structures and ARs receptors being one of the most targeted biological entities,<sup>4</sup> to date no drugs have been approved as agonists or antagonists of ARs.

Small molecules that interact with AR have been shown to be anti-inflammatory, cytotoxic, and modulators of neurological, cardiac and kidney diseases. In the early 1990s, an adenine derivative, N6-endonorbonan-2-yl-9-methyladenine (N-0861),<sup>5</sup> was introduced with great promise as an antagonist of adenosine receptors, but clinical trials did not yield the expected results. Since them other small molecules, in particular, xanthines have been used as *h*A<sub>1</sub>AR antagonists <sup>6</sup> in clinical trials. For instance, Biogen Inc. brought to clinical trials a xanthine derivative, tonapofylline (BG9928, ClinicalTrials.gov Identifier: NCT00745316, NCT00709865 & NCT00858156) for treating heart failure and renal insufficiency. Unfortunately, Biogen stopped the trials in phase 2b. While there have been great efforts to develop new *h*A<sub>1</sub>AR antagonist drugs, there are just few of them with high affinity for human A<sub>1</sub>AR (*h*A<sub>1</sub>AR) and high selectivity index over other *h*AR types <sup>7,8,9</sup>

Not only xanthine but also polysubstituted adenines have been shown to target AR. Some of them, as it was the case of SLV320, went into clinical trials<sup>10</sup> for treatment of congestive heart failure. Moreover, other groups, in particular the groups of Prof. Cristalli and Prof. Volpini have kept developing these chemotypes based on adenine as antagonists of AR.<sup>9,11</sup> In addition, the regulation of purinergic signalling contributes to several important pathologies such as cancer.<sup>3</sup>

Our group has focused on developing new synthetic methods to produce a wide range of polysubstituted purines. We introduced a one-pot synthesis of trisubstituted 6-alkoxypurines to obtain libraries with structural. 12,13,14 The use of these preciously developed libraries allowed us to identify key structural features of 6-alkoxy-purine analogues that induce programmed cell death in several types of cancer cell lines, in particular T cell cancer lines 15 and two novel purine-based chemotypes that could be further optimized to generate antiparasitic drugs against both *Plasmodium falciparum* and *Trypanosoma cruzi*. 12,16 Further to that, a novel synthetic route 17 for the synthesis of polysubstituted adenines was developed. Following this synthetic route, a library of small molecules was prepared and compounds with IC<sub>50</sub> values as low as 2.42 ± 0.16 mM, which target specific enzymes involved in purine metabolism within the parasite, were identified. 18

As these compounds were found to target enzymes of the trypanosome purine salvage pathway, whose ligands include adenine and adenosine, <sup>18</sup> we were interested in exploring whether this library might also exhibit affinity for human adenosine receptor subtypes, which also utilize adenosine as a natural ligand. Throughout the course of this project, our design strategy was further inspired by modifications of the adenine scaffold reported for the known *h*A<sub>1</sub>AR antagonist N-0861<sup>5</sup> and the work of Lambertucci.<sup>9</sup> Herein, we present our latest findings on the use of modified adenines as ligands of the *h*AR family, that showed potent binding for the *h*A<sub>1</sub>AR as well as antagonist activity in a cAMP assay. The interaction with the *h*A<sub>1</sub>AR was also simulated through docking computational analysis. We also investigated the cytotoxic effects of these modified adenine ligands on cancer cells, as there is evidence that the adenosine receptors play a role in cancer. <sup>11,19,20</sup>

#### 2. Material and methods

#### 2.1 Synthesis of purine library

Reaction courses and products mixtures where routinely monitored by TLC on silica gel Merck 60-200 mesh silica gel. Melting points were determined on a Stuart Scientific SMP3 apparatus and are incorrected. <sup>1</sup>H-NMR spectra were obtained in CDCl<sub>3</sub>, solution on a Varian Direct Drive (400 MHz and 500 MHz). Chemical shifts (δ) are given in ppm upfield from tetramethylsilane.

<sup>13</sup>C-NMR spectra were obtained in CDCl<sub>3</sub>, on a Varian Direct Drive (125 MHz). All products reported showed <sup>1</sup>H-NMR and <sup>13</sup>C-NMR spectra in agreement with the assigned structures. Mass spectra were obtained by electrospray (ES) with a LCT Premier XE Micromass Instrument (High resolution mass spectrometry). All final compounds are >95% pure by HPLC analysis (see Supporting Information).

The synthesis of compounds 11-15 (a-c) and their intermediates are described elsewhere. 18

### 2.1.1. General procedure for the preparation of compounds 7-10<sup>18</sup>

- A solution of 1 (7 mmol, 1 equiv.) in CH<sub>2</sub>Cl<sub>2</sub> (15 ml) containing TEA (initially 1.5 equivalents of each and in later reactions, when the disubstitution was checked, 2 equivalents). On this solution the different amines (10.54 mmol, 1.5 equiv. and later 2 equivalents) dissolved in CH<sub>2</sub>Cl<sub>2</sub> (5 mL) were added at room temperature for half an hour. Evaporation under vacuum gave a solid that was purified by column chromatography eluting with ethyl acetate/petroleum ether solutions.  $N^4$ ,  $N^6$ -di-tert-butyl-5-nitropyrimidine-4,6-diamine (7): Product 7, is not isolated, it is used as is for the following reaction.**4.1.3**. N<sup>4</sup>,N<sup>6</sup>-diethyl 5-nitropyrimidine-4,6-diamine (8): Yellow solid, yield 89%, mp: 85°C. δH (400.45 MHz, CDCl3): 9.29 (2H, bs, NH x2), 8.09 (1H, s, NCHN), 3.63 (4H, q, J=7.2 -CH2- x2), 1.28 (6H, t, J= 7.3, -CH3 x2). δC (100.70 MHz, CDCl3): 159.59, 157.16, 112.59, 36.38, 14.43. ES+HRMS: Calculated M+H=212.1147 C8H14N5O2. Obtained: 212.1148.
- 127
- 128 N<sup>4</sup>,N<sup>6</sup>-diisobutyl 5-nitropyrimidine-4,6-diamine (9): Yellow solid, yield 83%, mp: 78°C. δΗ
- 129 (400.45 MHz, CDCl3): 9.43 (2H, bs, NH x2), 8.05 (1H, s, NCHN), 3.42 (4H, dd, J=1.2 and 5.6 -
- 130 CH2- x2), 1.94 (2H, m, CH x2), 0.97 (12H, d, J= 3.9, -(CH3)2 x2). δC (100.70 MHz, CDCl3):
- 131 159.75, 157.67, 112.87, 48.99, 28.28, 20.29. ES+HRMS: Calculated M+H=268.1774
- 132 C12H22N5O2. Obtained: 268.1774.
- 133 N<sup>4</sup>,N<sup>6</sup>-diciclopentyl-5-nitropyrimidine-4,6-diamine (10): Yellow solid 76%, mp: 79°C. δΗ
- 134 (400.45 MHz, CDCl3): 9.37 (2H, bs, NH x2), 8.10 (1H, s, NCHN), 4.56 (2H, m, -CH cyclopentyl
- 135 x2), 2.69 (4H, m, -CH2 cyclopentyl x2), 1.77 (4H, m, -CH2 cyclopentyl x2), 1.67 (4H, m, -CH2
- 136 cyclopentyl x2), 1.53 (4H, m, -CH2 cyclopentyl x2). δC (100.70 MHz, CDCl3): 159.76, 157.05,

110

111

112

113

114

115

116

117

118

119

120

121

122

123

124

125

- 137 112.84, 53.29, 33.42, 23.87. ES+HRMS: Calculated M+H=292.1762 C14H22N5O2. Obtained:
- 138 292.1785.

#### 2.1.2. General procedure for the preparation of compounds 16-19:

- A solution of **7-10** (5 mmol, 1 equiv.) in EtOH (10 ml) containing SnCl<sub>2</sub> 2H<sub>2</sub>O (25 mmol, 5 equiv.),
- was refluxed for 1 h, monitoring the reaction by TLC. The mixture was then cooled at room
- temperature and NaHCO<sub>3</sub> was added until pH 8 was reached. After two extractions with EtOAc
- (10 ml for each one), the organic phase was washed with an aq. saturated solution of NaCl (2x25
- mL) and dried on Na<sub>2</sub>SO<sub>4</sub>. Evaporation under vacuum gave a solid that was purified by column
- chromatography eluting with ethyl acetate/petroleum ether solutions.
- 146 **N<sup>4</sup>,N<sup>6</sup>-di-tert-butylpyrimidine-4,5,6-triamine (16):** Pink solid, yield 43%. δH (400.45 MHz,
- 147 CDCl<sub>3</sub>): 8.04 (1H, s, NCHN), 3.88 ((2H, bs, NH x2), 1.44 (18H, s, -C(CH<sub>3</sub>)<sub>3</sub> x2).
- 148 **N<sup>4</sup>,N<sup>6</sup>-diethylpyrimidine-4,5,6-triamine (17):** Purple solid, yield 32 %, mp: 150°C. δH (400.45
- 149 MHz, CDCl3): 8.12 (1H, s, NCHN), 4.81 (2H, bs, NH x2), 3.46 (4H, q, J=7.2, -CH2- x2), 2.24 (2H,
- bs, NH2), 1.22 (6H, t, J= 7.2, -CH3 x2). δC (100.70 MHz, CDCl3): 157.84, 153.96, 101.19, 36.09,
- 151 15.66. ES+HRMS: Calculated M+H=182.1406 C8H16N5. Obtained: 182.1393.
- 152 **N<sup>4</sup>,N<sup>6</sup>-diisobutylpyrimidine-4,5,6-triamine (18):** Brown oil, yield 59 %. δH (400.45 MHz,
- 153 CDCl3): 8.09 (1H, s, NCHN), 5.00 (2H, bs, NH x2), 3.24 (4H, t, J=5.6 -CH2- x2), 2.14 (2H, bs,
- 154 NH2), 1.85 (2H, m, CH x2), 0.95 (12H, d, J= 5.4, -(CH3)2 x2). δC (100.70 MHz, CDCl3): 158.17,
- 153.76, 100.70, 48.76, 28.85, 20.37. ES+HRMS: Calculated M+H=238.2032 C12H24N5.
- 156 Obtained: 238.2026.
- 157 **N<sup>4</sup>,N<sup>6</sup>-dicyclopentylpyrimidine-4,5,6-triamine (19):** Purple solid, yield 45 %, mp: 265°C. δH
- 158 (400.45 MHz, CDCl3): 8.31 (2H, bs, NH x2), 8.12 (1H, s, NCHN), 4.33 (2H, m, -CH cyclopentyl
- 159 x2), 2.04 (4H, m, -CH2 cyclopentyl x2), 1.86 (8H, m, -CH2 cyclopentyl x2), 1.40 (4H, m, -CH2
- 160 cyclopentyl x2). δC (100.70 MHz, CDCl3): 159.76, 157.05, 112.84, 53.29, 33.42, 23.87.
- 161 ES+HRMS: Calculated M+H=262.2026 C14H24N5. Obtained: 262.2052.

162	2.1.3. General procedure for the preparation of compounds 16(a-c), 17c,
163	18c and 19c:
164	A solution of <b>16-19</b> (1 equiv.), with un excess (500 μL) of the corresponding trialkylorthoesthers or
165	triarylorthoesthers and methanesulfonic acid (0.2 equiv) was heated to 110°C for 24h, monitoring
166	the reaction by TLC. The mixture was then cooled at room temperature. After two extractions with
167	CH <sub>2</sub> Cl <sub>2</sub> the organic phase was washed with an aq. saturated solution of NaCl and dried on
168	Na <sub>2</sub> SO <sub>4</sub> . Evaporation under vacuum gave a solid that was purified by column chromatography
169	eluting with ethyl acetate/petroleum ether solutions.
170	<b>N,9-Di-</b> <i>tert</i> -butyl-9 <i>H</i> -purin-6-amine (16a). White solid, yield 83%, δH (400.45 MHz, CDCl <sub>3</sub> ): 8.34
171	(s, 1H), 7.76 (s, 1H), 5.71 (bs, 1H), 1.76 (s, 9H), 1.55 (s, 9H). δC (100.70 MHz, CDCl <sub>3</sub> ): 154.89,
172	151.62, 149.11, 136.88, 121.68, 57.24, 52.24, 29.30, 29.20. ES+HRMS: Calculated
173	M+H=248.1875 C <sub>13</sub> H <sub>22</sub> N <sub>5</sub> . Obtained 248.1862.
174	<b>N,9-Di-</b> <i>tert</i> -butyl-8-methyl-9 <i>H</i> -purin-6-amine (16b). Yellow solid, yield 28%, δH (400.45 MHz,
175	CDCl <sub>3</sub> ): $\delta$ 8.30 (s, 1H), 5.69 (bs, 1H), 2.73 (s, 3H), 1.85 (s, 9H), 1.55 (s, 9H). $\delta$ C (100.70 MHz,
176	CDCl <sub>3</sub> ): 153.90, 151.15, 150.85, 147.99, 123.57, 60.04, 52.20, 30.56, 29.35, 19.99. ES+HRMS:
177	Calculated M+H=262.2032 C <sub>14</sub> H <sub>24</sub> N <sub>5</sub> . Obtained: 262.2029.
178	<b>N,9-Di-tert-butyl 8-phenyl-9H-purin-6-amine (16c):</b> Yellow solid, yield 80%, bp: 100°C. δH
179	(400.45 MHz, CDCl <sub>3</sub> ): 8.39 (1H, s, NCHN), 7.52-7.40 57 (5H, m, Ph), 5.78 (1H, bs, NH), 1.63 (9H
180	s), 1.55 (9H, s). δC (100.70 MHz, CDCl <sub>3</sub> ): 151.30, 129.95, 129.59, 128.22, 60.46, 52.28, 49.82,
181	31.03, 29.31. ES+HRMS: Calculated M+H=324.2188 C <sub>19</sub> H <sub>26</sub> N <sub>5</sub> . Obtained: 324.2164.
182	<b>N,9-Diethyl-8-phenyl-9H-purin-6-amine (17c):</b> Yellow solid, yield 38 %, bp: 108° C. δH (400.45
183	MHz, CDCl3): 8.41 (1H, s, NCHN), 7.67 (2H, m, Ph), 7.52 (3H, m, Ph), 4.31 (2H, q, J=7.1 and
184	7.3, N-CH2), 3.73 (2H, m, NH-CH2), 1.42 (3H, t, J=7.2, -CH3), 1.33 (3H, t, J=7.2, -CH3). δC
185	(100.70 MHz, CDCl3): 150.52, 147.33, 132.07, 130.20, 129.09, 127.49, 119.64, 39.00, 29.83,
186	15.57, 15.17. ES+HRMS: Calculated M+H=268.1774 C15H18N5. Obtained: 268.1757.
187	<b>N,9-Diisobutyl-8-phenyl-9H-purin-6-amine (18c):</b> White solid, yield 57 %, bp: 155°C. δΗ
188	(400.45 MHz, CDCl3): 8.41 (1H, s, NCHN), 7.64 (2H, m, Ph), 7.51 (3H, m, Ph), 5.85 (1H, bs,
189	NH), 4.13 (2H, d, J=7.6, N-CH2), 3.49 (2H, bs, NH-CH2), 2.06 (1H, m, CH(CH3)2), 1.98 (1H, m,

- 190 CH(CH3)2), 1.02 (6H, d, J=6.7, -CH(CH3)2), 0.73 (6H, d, J=6.7, -CH(CH3)2). δC (100.70 MHz,
- 191 CDCl3): 155.06, 152.93, 150. 94, 130.82, 129.99, 129.03, 119.59, 50.91, 48.34, 28.81, 28.69,
- 192 20.40, 19.91. ES+HRMS: Calculated M+H=324.2188 C19H26N5. Obtained: 324.2169.
- 193 **N,9-dicyclopentyl-8-phenyl-9H-purin-6-amine (19c):** White solid, yield 28%, bp: 67°C. δΗ
- 194 (400.45 MHz, CDCl3): 8.39 (1H, s, NCHN), 7.59 (2H, m, Ph), 7.52 (3H, m, Ph), 5.80 (1H, bs, NH),
- 195 4.69 (2H, m, CH cyclopentyl), 2.57 (2H, m, CH2 cyclopentyl), 2.07 (4H, m, CH2 cyclopentyl),
- 196 1.98 (2H, m, CH2 cyclopentyl), 1.63(8H, m, CH2 cyclopentyl). δC (100.70 MHz, CDCl3): 154.47,
- 197 151.11, 150.13, 130.76, 129.96, 129.48, 128.95, 120.30, 58.06, 49.80 33.53, 31.02, 24.75, 23.81.
- 198 ES+HRMS: Calculated M+H=348.2182 C21H26N5. Obtained: 348.

#### 2.2 Biological assays

199

200

201

202

203

204

205

206

207

208

209

210

211

212

213

214

215

#### 2.1.4. Competition binding in hA1AR

*h*A<sub>1</sub>AR competition binding experiments were carried out in a multiscreen GF/C 96-well plate (Millipore, Madrid, Spain) pretreated with binding buffer (Hepes 20 mM, NaCl 100 mM, MgCl<sub>2</sub> 10 mM, adenosine deaminase 2 U/mL, pH=7.4). In each well was incubated 5 μg of membranes from Euroscreen CHO-A<sub>1</sub> cell line and prepared in our laboratory (Lot: A002/13-04-2011, protein concentration=5864 μg/ml), 1 nM [³H]-DPCPX (140 Ci/mmol, 1 mCi/mL, PerkinElmer NET974001MC) and compounds studied. Non-specific binding was determined in the presence of 10 μM R-PIA (Sigma P4532). The reaction mixture (Vt: 200 μL/well) was incubated at 25°C for 60 min, after was filtered and washed four times with 250 μL wash buffer (Hepes 20 mM, NaCl 100 mM, MgCl<sub>2</sub> 10 mM pH=7.4), before measuring radioactivity in a microplate beta scintillation counter (Microbeta Trilux, PerkinElmer, Madrid, Spain). Data was fitted to a 4-parameter logistic curve with GraphPad Prism 10 and K<sub>i</sub> values were derived from the Cheng-Prussof equation.<sup>21</sup>

#### 2.1.5. Competition binding in $hA_{2A}AR$

hA<sub>2A</sub>AR competition binding experiments were carried out in a multiscreen GF/C 96-well plate (Millipore, Madrid, Spain) pretreated with binding buffer (Tris-HCl 50 mM, EDTA 1 mM, MgCl<sub>2</sub> 10 mM, adenosine deaminase 2 U/mL, pH=7.4). In each well was incubated 5 μg of membranes

from Hela-A<sub>2A</sub> cell line and prepared in our laboratory (Lot: A002/17-04-2018, protein concentration=2058 μg/mL), 3 nM [³H]-ZM241385 (50 Ci/mmol, 1 mCi/mL, ARC-ITISA 0884) and compounds studied. Non-specific binding was determined in the presence of 50 μM NECA (Sigma E2387). The reaction mixture (Vt: 200 μL/well) was incubated at 25°C for 30 min, after was filtered and washed four times with 250 μL wash buffer (Tris-HCl 50 mM, EDTA 1 mM, MgCl<sub>2</sub> 10 mM, pH=7.4), before measuring radioactivity in a microplate beta scintillation counter (Microbeta Trilux, PerkinElmer, Madrid, Spain). Data was fitted to a 4-parameter logistic curve with GraphPad Prism 10 and K<sub>i</sub> values were derived from the Cheng-Prussof equation.<sup>21</sup>

#### 2.1.6. Competition binding in hA<sub>2B</sub>AR

 $hA_{2B}$ AR competition binding experiments were carried out in a multiscreen GF/C 96-well plate. In each well was incubated 25 μg of membranes from Euroscreen HEK-A<sub>2B</sub> cell line and prepared in our laboratory (Lot: A009/14-02-2020, protein concentration=5254.8 μg/mL), 25 nM [³H]-DPCPX (137 Ci/mmol, 1 mCi/mL, PerkinElmer NET974001MC) and compounds studied. Non-specific binding was determined in the presence of 1000 μM NECA (Sigma E2397). The reaction mixture (Vt: 250 μL/well) was incubated at 25°C for 30 min, 200 μL was transferred to GF/C 96-well plate (Millipore, Madrid, Spain) pretreated with binding buffer (Tris-HCl 50 Mm, EDTA 1 mM, MgCl<sub>2</sub> 5 mM, Bacitracin 100 μg/μL, adenosine deaminase 2 U/mL, pH=6.5), after was filtered and washed four times with 250 μL wash buffer (Tris-HCl 50 mM, EDTA 1 mM, MgCl<sub>2</sub> 5 mM, pH=6.5), before measuring radioactivity in a microplate beta scintillation counter (Microbeta Trilux, PerkinElmer, Madrid, Spain). Data was fitted to a 4-parameter logistic curve with GraphPad Prism 10 and K<sub>i</sub> values were derived from the Cheng-Prussof equation.<sup>21</sup>

#### 2.1.7. Competition binding in hA<sub>3</sub>AR

hA<sub>3</sub>AR competition binding experiments were carried out in a multiscreen GF/B 96-well plate (Millipore, Madrid, Spain) pretreated with binding buffer (Tris-HCl 50 mM, EDTA 1 mM, MgCl<sub>2</sub> 5 mM, adenosine deaminase 2 U/mL, pH=7.4). In each well was incubated 30 μg of membranes from Hela-A<sub>3</sub> cell line and prepared in our laboratory (Lot: A006/17-01-2020, protein concentration=3408 μg/mL), 10 nM [³H]-NECA (22.4 Ci/mmol, 1 mCi/mL, PerkinElmer

NET811250UC) and compounds studied. Non-specific binding was determined in the presence of 100 μM R-PIA (Sigma P4532). The reaction mixture (Vt: 200 μL/well) was incubated at 25°C for 180 min, after was filtered and washed six times with 250 μL wash buffer (Tris-HCI 50mM pH=7.4), before measuring radioactivity in a microplate beta scintillation counter (Microbeta Trilux, PerkinElmer, Madrid, Spain). Data was fitted to a 4-parameter logistic curve with GraphPad Prism 10 and K<sub>i</sub> values were derived from the Cheng-Prussof equation.<sup>21</sup> The conditions were carried out in triplicate.

#### 2.1.8. Functional study of seven adenine derivatives (Table 2) in hA1AR

*h*A<sub>1</sub>AR functional experiments were carried out in CHO-A<sub>1</sub> cell line. The day before the assay, the cells were seeded on the 96 well culture plate (Falcon 353072). The cells were washed with wash buffer (Nutrient Mixture F12 Ham's (Sigma N6658), 25mM Hepes; pH=7.4). Wash buffer was replaced by incubation buffer (Mixture F12 Ham's (Sigma N6658), 25mM Hepes, 20 μM Rolipram (Sigma R6520); pH=7.4). Test compounds and XAC as reference compound (Sigma X103) were added and incubated at 37°C for 15 min. After, a concentration response curve of 5'-(*N*-ethylcarboxamido)adenosine (NECA) (Sigma E2387) was added and incubated at 37°C for 10 min. 10 μM FSK (Sigma F3917) was added and incubated at 37°C for 5 min. After incubation, the amount of cAMP is determined using *cAMP Biotrak Enzymeimmunoassay (EIA) System Kit* (GE Healthcare RPN225). Data was fitted to a 4-parameter logistic curve with GraphPad Prism 10 and K<sub>B</sub> values were derived from the derivation of Cheng-Prusoff equation proposed by Leff and Dougall.<sup>22</sup> The conditions were carried out in triplicate.

#### 2.1.9. Cell based assays

Adherent HCT-116, HKH2 (HCT116 with KRAS knockout), SW480, SW48, A549, MDA-MB-231 and MCF7 cells were maintained in DMEM supplemented with 10% FBS, and 2mM L-Glutamine, and incubated at 5% CO2 at 37°C in a Heracell 240i tissue culture incubator. Semi-adherent K562 cells were maintained in RPMI 1640 supplemented with 10% FBS, and incubated at 5% CO<sub>2</sub> at 37°C in a Heracell 240i tissue culture incubator. Cells were passaged when 80-90% confluent for maintenance

#### 2.1.10. Phenotypic screening

270

271

272

273

274

275

276

277

278

279

280

281

282

283

284

285

286

287

288

289

290

291

292

293

294

295

296

Cells were seeded into 96-well plates at the following densities with a working volume of 100µL: HCT116, SW480, HKH2, MDA-MB-231, MCF7, and A549 at 1000 cells/well, and SW48 at 4500 cells/well. K562 cells were seeded at 3000 cells/well, in a 95µL working volume. Seeding densities were decided using prior seeding density assays. All plates were incubated for 2 days, prior to treatment, apart from K562 which was seeded and treated on the same day. Drugs were prepared in DMSO with a working volume of 50µL with a concentration range from 100mM -0.001mM, by serial dilution. To dilute drugs to the desired concentrations before adding to the cell plates, intermediate plates were freshly prepared, using 245µL of DMEM and RPMI media and 5μL of drug at each concentration. 5μL of this solution was then added to 95μL media in the cell plate to achieve a final dilution of 1000x and 0.01% DMSO from the initial drug plates. On day 2, media was aspirated and replaced with 95µL fresh media before adding 5µL of each drug from freshly prepared intermediate plates. Plates were then incubated for a further 5 days for drug treatment. Prestoblue dye was added to an additional seeded cell plate for each cell line to normalize for viability from the 2-day incubation. Prestoblue dye was incubated for 90 minutes. After incubation, absorbance was read on a PerkinElmer Envision 2101 plate reader at an emission wavelength of 580 nm. After 5 days of drug treatment, all plates were incubated with Prestoblue. All drug concentrations were transformed into logarithmic scales, with all conditions being converted into percentage viability compared to untreated cells (100% viability). Percentage viability values were used to calculate EC50 values for each condition, using non-linear regression variable slope (four parameters) in GraphPad Prism 9. The conditions were carried out in triplicate.

#### 2.3 Docking Protocol

Docking analysis was carried out with Autodock 4.2.6 (AD4)<sup>23</sup> on the  $hA_1AR$  ( $hA_1AR$ , pdb IDs 5UEN, subunit B) and  $hA_{2A}AR$  ( $hA_{2A}AR$ , pdb IDs 4EIY). Ligands structures were built on Avogadro<sup>24</sup> and optimized using Gaussian software (HF/6-31G(d,p)) [Frisch et al. 2009].<sup>25</sup> Once optimized, ligands PDB files were prepared for docking using the prepare\_ligand4.py script

included MGLTools 1.5.4.<sup>23</sup> Protein structure, were prepared for docking using the PDB2PQR tools.<sup>26</sup> Water and ligand molecules were removed and charges and non-polar hydrogen atoms were added at pH 7.0. The produced structures were saved as a pdb files and prepared for docking using the prepare\_receptor4.py script from MGLTools. AD4 was used to dock the ligands into the *h*A<sub>1</sub> and *h*A<sub>2A</sub>AR orthosteric binding site. The docking grid was centered on the orthosteric site and set with the following grid parameters: 70 Å × 60 Å × 70 Å with 0.375 Å spacing. In all calculations, AD4 parameter file was set to 100 GA runs, 2.500.000 energy evaluations and a population size of 150. The Lamarckian genetic algorithm local search (GALS) method was used for the docking calculations. All dockings were performed with a population size of 250 and a Solis and Wets local search of 300 rounds was applied with a probability of 0.06. A mutation rate of 0.02 and a crossover rate of 0.8 were used. The docking results from each of the 100 calculations were clustered based on root-mean square deviation (RMSD) solutions differing by less than 2.0 Å between the Cartesian coordinates of the atoms and ranked based on free energy of binding. The obtained conformations were individually inspected and figures were created with UCSF Chimera 1.15 [Pettersen et al. 2004].<sup>27</sup>

#### 3. Results

#### 3.1 Synthesis of N-6,8,9-trisubstituted adenines

The commercially available compound 4,6-dichloro-5-nitropyrimidine was employed as the starting material to obtain the propargyloxy-substituted pyrimidine 1 in good yield through a reaction with propargyloxy alcohol. Subsequently, pyrimidine 1 was reacted with primary amines at room temperature, giving rise, initially, to the symmetric disubstituted 4,6-bis(alkyl/arylalkyl)amino-5-nitropyrimidines 2-7 via pre-reactive molecular complexes. The reduction of these pyrimidines was performed using tin(II) chloride, resulting in the formation of 4,6-bis(alkyl/arylalkyl)amino-5-aminopyrimidines 11-15. These compounds were cyclized with three distinct trialkyl orthoesters (trimethyl orthoformate, trimethyl orthoacetate, or trimethyl orthobenzoate) and methanesulfonic acid (Scheme 1) to obtain purines with H (family a), methyl

(family b) and phenyl (family c) at C8 (Scheme 1) to obtain their derivatives **11a-15c**, that were previously presented by our group as antiparasitic compounds. <sup>18</sup> For the purposes of the present study, we expanded the library of compounds to include derivatives with a tert-butyl group, an ethyl group, an isobutyl group and a cyclopentyl group in positions 6 and 9. The synthesis of these novel compounds, specifically **16c**, **17c**, **18c**, and **19c**, was achieved via cyclization with trimethyl orthobenzoate to obtain purines with phenyl (family c) at C8 (Scheme 1).

All compounds were purified by column chromatography and characterised by nuclear magnetic resonance (<sup>1</sup>H-NMR and <sup>13</sup>C-NMR), high-resolution mass spectrometry (HRMS) and HPLC. As illustrated in Figure 1, the synthesised compounds share a purine ring, presenting two substituents at positions C6/N9, containing either aromatic or non-aromatic chains, and a substituent at C8.

## 3.2 Evaluation of the binding affinities of the purine library to $hA_1$ , $hA_2A$ , $hA_2B$ and $hA_3$ ARs.

A series of seventeen adenine derivatives was evaluated *in vitro* for affinity and selectivity against the four *h*AR, using radioligand binding assays (Table 1). Biological results are expressed as K<sub>1</sub> (nM, n = 3) or as percentage inhibition of specific binding at 10 μM (n = 2, average) for those compounds that did not fully display specific radioligand binding. K<sub>1</sub> values were obtained by nonlinear regression fitting of the data using Prism 7.0 software (GraphPad, San Diego, CA). Four known *h*AR ligands (XAC, CGS-15943, ZM241385, and MRS1220) were used as reference compounds, and the results are shown in Table 1.

Out of the seventeen compounds, four compounds stood out due to their affinity for one or two ARs. All these four compounds (**11c**, **12c**, **14c** and **15c**, Figure 1) shared a common structural feature, a phenyl group at position 8 of the adenine scaffold. 6/9-Bisarylalkyl derivatives, such as *N*,9-diphenethyl-8-phenyl-9*H*-purin-6-amine (**12c**) and *N*,9-bis(4-chlorobenzyl)-8-phenyl-9*H*-purin-6-amine (**15c**), proved to be selective against *h*A<sub>1</sub>AR, with low percentages of inhibition of the three other ARs at 10 μM, the highest concentration tested. The dibenzyl derivative without substituents on the aromatic rings at positions C6 and N9, *N*,9-dibenzyl-8-phenyl-9H-purin-6-

amine (**11c**) showed a dual profile as  $hA_1/hA_{2B}AR$  ligand, with a selectivity index of 2.4. This is the only molecule within the series that can be considered a dual  $hA_1/hA_{2B}AR$  ligand ( $K_i = 458.8$  nM and 1091 nM, respectively).

Out of the two 6/9-bisalkyl derivatives, N,9-diisopropyl-8-phenyl-9H-purin-6-amine (**14c**) proved to be the most active compound within the series, with a  $hA_1AR$   $K_i$  of 2.0±0.3 nM (Table 1). This compound showed an affinity for the  $hA_3AR$ , with a  $K_i$  of 211.2±53 nM, meaning a selectivity index of 105.6. Therefore, **14c** was considered as a  $hA_1AR$  selective ligand. Compound **16c**, a similar compound than **14c** but with a tert-butyl substituent rather than isopropyl at C6 and N9, was found to be non-active.

### 3.3 Evaluation of the antagonist potency (K<sub>B</sub>) of the best ligands to hA₁AR.

From the initial screening, it was clear that the most promising compounds had a very specific and selective interaction with  $hA_1AR$ . Therefore, the four most active compounds (11c, 12c, 14c and 15c, Figure 1) were selected to further investigate whether they act as agonists or antagonists of  $hA_1AR$ , using a cAMP assay. The results of the  $hA_1AR$  adenosinergic profile are shown in Table 2.

These results clearly show that compound **14c**, with isopropyl substituents, is the most promising candidate due to its low  $K_B$  value, indicating higher potency as an antagonist against the  $hA_1AR$ .

#### 3.4 Evaluation of new compounds based on 14c as lead compound

Adenine **14c** was thus chosen as the lead compound from the library presented above, and the influence of the alkyl substituents at C6 and N9 in this scaffold was further investigated, while keeping the phenyl group at position 8, which is critical for maintaining activity. Derivatives **17c** and **18c** were then synthesized, using the same synthetic pathway shown above (Scheme 1) to introduce ethyl and isobutyl substituents at these positions as less bulky groups than *tert*-butyl. Moreover, the *N*,9-dicyclopentyl-8-phenyl-9H-purin-6-amine (**19c**, Figure 2) was synthesised based on N6-endonorbonan-2-yl-9-methyladenine (**N-0861**), which was developed in the early 1990s [Shryock et al. 1992; Pelleg & Hurt 1992];<sup>5,28</sup> and the most recent work by Lambertucci et

al.,<sup>9</sup> which reports that these scaffolds, containing a cycloalkylamine substituent at C6 (Figure 2), were found to be antagonists of *h*A1AR with IC<sub>50</sub> values at the nanomolar level.

After successfully synthesizing the three new compounds (Figure 2), they were screened for binding affinity to the four *h*ARs (A<sub>1</sub>, A<sub>2</sub>A, A<sub>2B</sub>, and A<sub>3</sub>). The three compounds have a K<sub>1</sub> for *h*A<sub>1</sub>AR below 50 nM (Table 1), which is the lowest within the whole library, along with their lead compound **14c**. Furthermore, **19c**, which contains cyclopentyl substituents, exhibits high specificity for *h*A<sub>1</sub>AR with very low affinity for the three remaining *h*ARs at 10 μM. In contrast, **17c** and **18c** exhibit K<sub>1</sub> values in the low micromolar range against some of the other receptors, indicating that **19c** has the highest binding specificity of the compounds presented here towards *h*A<sub>1</sub>AR among all the adenosine receptors. Finally, their antagonist potency (K<sub>B</sub>) against *h*A<sub>1</sub>AR was measured showing values below 100 nM for **17c**, **18c** and **19c** (Table 2).

Having established that the bisalkyl-substituted purines with a phenyl in position 8 of the purine ring have the highest affinity and antagonist activity for *h*A<sub>1</sub>AR, we decided to phenotypically screen them against several cell lines to determine their antiproliferative activity.

## 3.5 Phenotypic screening for antiproliferative effects across six different cell

#### lines

To study the antiproliferative effects of the four bisalkyl-substituted purines, we selected six different cell lines shown in Table 3. Each of these cell lines provides a good model for testing the efficacy of anticancer drugs against highly prevalent cancers such as colon, breast, lung and leukaemia.

Table 4 presents the antiproliferative  $EC_{50}$  values in micromolar concentrations. **19c** showed significant potency across all tested cell lines, with the lowest  $EC_{50}$  value of 7  $\mu$ M observed in SW480 cells. The range of  $EC_{50}$  values, varying from 7  $\mu$ M to 39  $\mu$ M, across different cell lines. On the other hand, **18c** showed high  $EC_{50}$  values in most cell lines, except for SW-480 and K562, where they had lower  $EC_{50}$  values of 13  $\mu$ M and 17  $\mu$ M, respectively. Finally, **17c** presented very

low or no antiproliferative activity in most cell lines, except in the case of MDA-MB-231, which had a moderately low EC $_{50}$  value of 30  $\mu$ M.

# 3.6 Correlation analysis of mRNA expression and sensitivity to lead compound 19c using RNAseq data from DepMap

To understand whether the antiproliferative effects of the lead compound **19c** are due to its antagonistic action on hA1ARs, a correlation analysis was carried out. The analysis looked at the relationship between ADORA1 mRNA expression levels, which encode the adenosine hA1AR, across various cell lines (Table 3) and their sensitivity to **19c**. The expression data were sourced from RNAseq datasets provided by the DepMap project.

The results obtained are shown in Figure 3A, which shows scatter plots with linear regression lines, representing the relationship between ADORA1 expression levels and the log-transformed EC<sub>50</sub> of **19c**. Although there was a negative correlation observed in both cases (R = -0.57, p = 0.24; R = -0.47, p = 0.29), the associations did not reach statistical significance.

On the other hand, Figure 3B shows a boxplot where cell lines are stratified by median expression levels of ADORA1, categorized into 'Low' and 'High' expression groups based on median cutoff values (left = 217, right = 131). T-tests indicate no statistically significant difference in compound sensitivity between the two groups (left p-value = 0.2318, right p-value = 0.1966).

#### 3.7 Molecular Modelling

Based on our screenings, we established that a phenyl ring at the 8th position and alkyl groups at the 6th and 9th positions on the adenine scaffold are significant for selective antagonism of the  $hA_1AR$ . Specifically, adenine with substituents of either isopropylamine or cyclopentyl at positions 6 and 9 showed high binding affinity and selectivity towards  $hA_1AR$ . This suggests an optimal fit within the  $hA_1AR$  binding pocket. To explain the molecular basis of this interaction, we performed docking simulations to investigate the specific interaction between the ligand and receptor. The best performing compounds, **14c** and **19c**, were thus investigated to assess the molecular interactions of these compounds in the  $A_1$  subtype G-protein-coupled receptor ( $hA_1AR$ ) and the  $A_{2A}$  subtype. The crystal structure of  $hA_1AR$  (PDB ID: 5UEN) was chosen to perform the docking

analysis [Glukhova et al. 2017]. This structure represents an inactive conformation of  $hA_1AR$  with a covalently-bound selective antagonist (DU172), and exhibits an open site binding cavity capable of accommodating both orthosteric and allosteric ligands. The preferred binding pose of **14c** on hA₁AR (PDB ID: 5UEN) is shown in Figure 4a. The adenine ring is set between Leu250 and Phe171 forming stacking interactions with both residues and matching the binding orientation seen on the adenine moiety of the natural agonist adenosine in the hA<sub>1</sub>AR active conformation (PDB ID: 7LD4) (Figure 4b) [Draper-Joyce et al. 2018; Draper-Joyce et al. 2021]. Similarly, this orientation allows the formation of a double H-bond interaction between the hydrogen of the 6-amine (hydrogen donor) and the N7 (hydrogen acceptor) in the adenine ring with the side chain of Asn254, as does adenosine in the hA₁AR active conformation (see PDB ID: 7LD4). In a similar way, antagonist DU172 in the inactive conformation (PDB ID: 5UEN) h-bond the side chain of Asn254 (Figure 4c), but in a different orientation when compared with adenine 14c binding pose. The C8 and N6 substituents at 14c, are both facing hydrophobic pockets that are closed on the active conformation of hA<sub>1</sub>AR (Figure 4d). The phenyl ring on C8 is displayed in the same region as the N1-propyl substituent in DU172, in a pocket deeper in the orthosteric site created by Val87, Thr91, Asn184, Thr277, Trp247, and His251, and shows a significant π-stacking interaction with Trp247. The side-chain movement of this residue, together with Val87, Thr91, Asn184, and Thr277, is responsible for the partial closure of this pocket on the hA₁AR active conformation. As for the N6-isopropyl substituent, it is displayed in a hydrophobic cleft towards the extracellular end of the receptor (Figure 4a and 4c). This cleft, located between helix5 (H5), helix6 (H6), and helix7 (H7), is also occupied by the cyclohexane moiety of cognate ligand DU172 and is established by residues Glu172, Met180, Leu253, Thr257 and Thr270. This last residue is hA1AR specific and has been suggested to act as a gatekeeper for ligand access to the orthosteric site [Cheng et al. 2017]. On the other hand, the isopropyl substituent at N9 on **14c** occupies the same position as the ribose ring of the adenosine in the *h*A₁AR active conformation (PDB ID: 7LD4), stablishing van der Waals interactions with Val87. In an identical manner, the most active compound, ligand 19c, adopts the same spatial arrangement as 14c on the inactive conformation of receptor hA<sub>1</sub>AR (Figure 4e). The difference between these two

430

431

432

433

434

435

436

437

438

439

440

441

442

443

444

445

446

447

448

449

450

451

452

453

454

455

456

ligands is their substituents at N6 and N9 with two isopropyl chains on <b>14c</b> and two cyclopentyl
rings on <b>19c</b> . The two, more voluminous and hydrophobic residues, on <b>19c</b> are inserted in the
pocket created by Val87, Thr91, Asn184, Thr277, Trp247, and His251, as well as in the
hydrophobic cleft between H5, H6, and H7, superimposing the spatial disposition of the isopropyl
substituents on <b>14c</b> . In both locations, the cyclopentyl rings stablish van der Waals interactions
with the residues involved (Figure 4e and 4f).
Only minor differences define the active and inactive conformation of hA1AR These are the
inward movement of transmembrane helix1 (H1) and helix2 (H2), upward movement of helix3
(H3), the displacement of H7 toward H6, and side-chain variations of Trp247, His278, Val87,
Leu88, Thr91 and Thr277 [Draper-Joyce et al. 2018]. As a result, the inactive conformation shows
a more open orthosteric binding site when compared to the active one. As described above, the
preferred docking poses of 19c and 14c take advantages of this open orthosteric binding site in
the inactive conformation, by inserting their N6 substituents in the hydrophobic cleft generated by
the extracellular outward movement of H7, and its C8-phenyl ring in the pocket generated by
residues Trp247, Val87, Leu88, and Thr91. Hence, this wider and more exposed orthosteric
binding site observed in the inactive conformation could explain the higher affinity of ligands 19c
and 14c toward this conformation that, in combination with the molecular interactions established
with important catalytic and conformational-dependent residues, might account for the
experimental low nanomolar $K_{i}$ values observed in this isozyme and its antagonist activity.
As for the differences between $A_1$ and $A_{2A}$ receptors, they are mainly focused on conformational
variations in the extracellular ends of H1, H2, H3, and H7, as well as the orientation of
extracellular loop 2 (ECL2). These differences determine that the extracellular region of the
orthosteric binding site on $hA_1AR$ is more open than that of $hA_{2A}AR$ . Some minor differences are
also found on their binding pockets, where only four residues change: Val62, Asn70, Glu170, and
Thr270 in hA <sub>1</sub> AR (corresponding to Ala59, Ser67, Leu170, and Met270 in hA <sub>2A</sub> AR) [Cheng et al.
2017]. When ligands <b>19c</b> and <b>14c</b> were docked on $hA_{2A}AR$ (PDB ID: 4EIY), an inactive
conformation of the receptor with antagonist ZM241385 bound to its orthosteric binding site,
substantially different bonding poses were found compared to those seen on <i>h</i> A₁AR. The adenine

ring is displayed with its C8 phenyl ring pointing towards a hydrophobic pocket located between H2 and H3 and enabled by the presence of the less bulky, hA<sub>2A</sub>AR specific, Ala59 residue at H2. Moreover, the inward movement of the extracellular end of H7 in  $hA_{2A}AR$  also prevents the  $hA_1AR$  adenine orientation, disallowing the H-bonds with Asn253 ( $hA_{2A}AR$  numbering) and an effective stacking interaction with Leu249 (Leu250 in hA1AR). In addition, the presence of the hA<sub>2A</sub>AR specific Met270 residue at H7 blocks the cleft that allowed the insertion of the N6isopropyl and cyclohexyl substituents in  $hA_1AR$ , forcing the adenine into the new orientation (Figure 5a and 5b). In summary, the different poses observed for ligands 19c and 14c on both receptors due to the extracellular conformational variations, as well as the receptor-specific binding site residues, could explain the experimentally observed isozyme selectivity in these ligands. The predicted binding energies and inhibitory constants of 19c, 14c and the natural ligand adenosine against 5UEN (hA1AR inactive), 7LD4 (hA1AR active), 4EIY (hA2AAR inactive) and 5G53 (hA2AAR active) are presented in Table SI-1. The data indicate that 19c is the most effective ligand in terms of binding strength and inhibitory potency among the proteins under study. These findings suggest that 19c may be a promising candidate for further drug development targeting these adenosine receptors.

## 3.8 Physicochemical and pharmacokinetic characterization of the adenine derivatives and reference standards

Finally, the adenine library and reference standards were characterized for their physicochemical and pharmacokinetic properties using chemical informatics tools to evaluate their potential as drug candidates. The total solvent-accessible surface area (TSPA), partition coefficient (cLogP), were calculated using the SwissADME web-based tools [Daina et al. 2017]. The TSPA and cLogP values provided insight into the molecules' size, shape and lipophilicity. Based on these results, we observed that despite sharing the same TSPA, modification of positions 6 and 9 in the purine ring have a great impact in the lipophilicity of the molecules and therefore can influence the absorption, distribution, metabolism, and excretion (ADME) profile of these compounds.

486

487

488

489

490

491

492

493

494

495

496

497

498

499

500

501

502

503

504

505

506

507

508

509

510

511

Next, the compounds and control molecules were further analyzed for their drug metabolism and pharmacokinetics (DMPK) properties using the pkCSM web tool.<sup>29</sup> Relevant DMPK parameters, including CaCo2 permeability, intestinal absorption, BBB permeability (log BB), fraction unbound (human) (Fu), and predicted clearance, were calculated. These parameters provided additional information about the compounds' bioavailability, distribution, and elimination characteristics. The parameters obtained for the four most promising compounds within the studied series are shown in Table SI-2. To analyse these results, we focused on **14c**, the compound with the lowest  $K_i$  and  $K_B$  for  $hA_1R$ , and 19c the highest selectivity index for hA<sub>1</sub>R and the best antiproliferative performance of the entire library presented here. The pharmacokinetic profiles of these two compounds present several similarities. Both compounds exhibit an identical TPSA of 55.63 Ų as well as very similar high intestinal absorption rates. However, there are also notable differences. Compound 14c present a higher CaCo2 permeability (1.32 Log Papp) in comparison to **19c** (0.64 Log Papp). indicating a superior intestinal permeability. On the other hand, 19c present markedly elevated blood-brain barrier (BBB) permeability (0.78 Log BB) in comparison to **14c** (-0.03 Log BB), indicating a greater chance for 19c to go through the BBB. Furthermore, 19c shows a higher fraction unbound (0.42) in comparison to 14c (0.17), indicating that a greater proportion of 19c is present in its free form. Lastly, 19c has a higher predicted clearance (0.82 log ml/min/kg) than **14c** (0.59 log ml/min/kg), indicating a potentially more rapid clearance from the body

531532

533

534

535

536

537

538

513

514

515

516

517

518

519

520

521

522

523

524

525

526

527

528

529

530

#### 4. Discussion

The described synthetic route provides access to a library of eighteen 6,8,9-trisubstituted adenine derivatives, demonstrating structural diversity generated through an efficient cyclization reaction. To note, the formation of 4,6-bis(alkyl/arylalkyl)amino-5-nitropyrimidines (**2-7**) via pre-reactive molecular complexes, a phenomenon that has rarely been reported in SNAr reactions. This finding was recently presented by our research.<sup>17</sup>

Given that our compounds were initially designed to target enzymes of the trypanosome purine salvage pathway, a metabolic pathway that relies on adenine and adenosine as substrates we hypothesized that they might also have affinity for human adenosine receptors, which also use adenine as a natural ligand. This hypothesis led us to investigate the interaction of these compounds with hAR subtypes. Therefore, we began this study by screening our previously published library of compounds, including molecules 11a-15c, to interrogate their binding affinity toward the four human adenosine receptor subtypes (A<sub>1</sub>, A<sub>2A</sub>, A<sub>2B</sub>, and A<sub>3</sub>). 18 This initial screen identified several compounds with interesting affinity and selectivity profiles for hARs (Table 1). In particular, the presence of a phenyl group at position C8 was demonstrated to be crucial for obtaining high-affinity ligands for hA<sub>1</sub>AR. Moreover, the nature of the substituents at positions 6 and 9 was found to be important for achieving selectivity, as bisarylalkyl derivatives such as 12c and **15c** showed selective binding affinity towards hA<sub>1</sub>AR. The dibenzyl derivative without substituents on the aromatic rings **11c** showed a dual profile for hA<sub>1</sub>AR and hA<sub>2B</sub>AR subtypes. Among the bisalkyl derivatives, compound **14c**, with isopropyl substituents at positions 6 and 9, was identified as the most potent binder, with a Ki of 2 nM, lower than that obtained with reference compound XAC, and a selectivity index of 105.6 against the hA<sub>3</sub>AR receptor subtype. To our knowledge, **14c** is the most potent *h*A<sub>1</sub>AR binder described to date. Functional studies of the most promising candidates confirmed that these molecules acted as antagonists at the  $hA_1AR$ . In addition, using compound **14c** as the lead structure and based on previous work with hA<sub>1</sub>AR antagonists and inspired by N-0861<sup>5,28</sup> and the work of Lambertucci,<sup>9</sup> that presented cycloalkyl groups at N6 of the adenine ring four new derivatives, 16c, 17c, 18c and 19c, were designed and synthesized. Compound 19c, containing two cyclopentyl groups showed the highest binding affinity of the three new compounds to the hA1AR, with K<sub>i</sub> below 50 nM. Importantly, compound **19c** presented a very high selectivity for the *h*A₁AR over the other AR subtypes, confirming the importance of the substituents at positions 6 and 9 for the selectivity profile. In addition, these new compounds presented K<sub>b</sub> values below 100 nM, thus indicating them as very promising lead compounds.

539

540

541

542

543

544

545

546

547

548

549

550

551

552

553

554

555

556

557

558

559

560

561

562

563

564

The phenotypic screening (Table 4) of the most promising compounds (14c, 17c, 18c and 19c) across six different human cell lines (Table 3) revealed that compound 19c had an interesting antiproliferative effect, exhibiting the lowest EC<sub>50</sub> values, and a particularly strong effect on SW480, a colorectal cancer cell line, for which an EC<sub>50</sub> of 7 µM was determined. When comparing the EC<sub>50</sub> values of **19c** and **14c** across the six cancer cell lines, both compounds exhibit antiproliferative activity. However, 19c consistently shows greater potency. The similar proportional effect of **14c** and **19c** across the cell lines could suggest that they target similar pathways, with **19c** being more effective at inhibiting those pathways. The difference in efficacy between 19c and 14c may be due to several factors, such as 19c higher affinity for the target in the cellular environment or better cellular uptake. It is also possible that 19c engages additional targets or pathways contributing to its enhanced potency. These results indicate that this type of bisalkyl-substituted adenines can be further developed as potential anticancer agents, with a focus on colorectal cancer models. Further mechanistic studies would then be required. In contrast, 18c, and especially 17c, had poor or no antiproliferative activity in most of the cell lines. While not achieving statistical significance, a trend towards a negative correlation between ADORA1 mRNA expression and the sensitivity to compound 19c was observed. This result suggests that ADORA1 expression may potentially serve as a biomarker for responsiveness to these families of compounds, although further investigation with more cell lines and samples would be necessary to confirm this potentiality. Molecular modelling studies suggest that the adenine ring is stabilized by stacking interactions with Leu250 and Phe171, while the N6 and C8 substituents interact with specific residues within the orthosteric pocket. The binding orientation seen on the adenine moiety matches that of the natural agonist adenosine. Importantly, the N6-isopropyl group of **14c** and the N9-isopropyl group of **14c** occupied analogous positions to the ribose and the cyclohexane moiety of known hA₁AR ligands, which suggests a role for these groups in the binding process. The higher activity of 19c, with cyclopentyl substituents, could be due to the higher hydrophobicity and volume of these

566

567

568

569

570

571

572

573

574

575

576

577

578

579

580

581

582

583

584

585

586

587

588

589

590

groups, as they occupied the same pocket as the isopropyl substituents in 14c, but with stronger van der Waals interactions with surrounding residues. Differences in binding poses in the hA<sub>1</sub>AR and the hA<sub>2A</sub>AR receptors could be attributed to conformational variations and the different specific residues of their orthosteric binding sites. For example, the extracellular end of H7 in hA<sub>2A</sub>AR prevents the adenine orientation seen in the  $hA_1AR$ , while a more opened hydrophobic pocket, which is specific to the  $A_{2A}$  subtype, allows the phenyl group to fit. The different binding poses observed are consistent with the observed selectivity profile. While our modeling studies suggest the positioning of the substituents within the receptor binding site, additional experimental data is required to confirm those interactions, as well as the preferred poses of the various molecules. Finally, the in silico analysis of the physicochemical and pharmacokinetic profiles of these compounds suggested that both 14c and 19c may be potentially useful for drug development, presenting a good balance between their absorption, distribution, metabolism and excretion profiles, and showing high intestinal absorption rates. These properties suggest that 14c and 19c may be a potentially useful compound for further development as drug candidates with excellent oral bioavailability.

609

610

611

612

613

614

615

616

593

594

595

596

597

598

599

600

601

602

603

604

605

606

607

608

#### 5. Conclusion

In summary, the results presented here highlight the potential of trisubstituted adenine derivatives as high-affinity and highly selective  $hA_1AR$  antagonists. The identification of  $\mathbf{19c}$  as a potent and selective  $hA_1AR$  antagonist, with good bioavailability and significant antiproliferative effects, provides a strong foundation for further optimization and development of a new family of AR ligands. The data obtained in docking simulations also suggest that ligand  $\mathbf{19c}$  may be a promising candidate for further drug development targeting these adenosine receptors. These compounds, and particularly compound  $\mathbf{19c}$ , show promise for future therapeutic applications.

618

## 6. Acknowledgments

620 M.J.M. thanks Ministerio de Ciencia e Innovación (PID2020-116076RJ-

I00/AEI/10.13039/501100011033) for the financial support. The authors thank the Centro de

Servicios de Informática y Redes de Comunicación (CSIRC), Universidad de Granada, for

623 providing the computing time. Funding for open access charge: Universidad de Granada / CBUA

624

621

622

625

626

627

#### 7. Disclosure

The author(s) report no conflicts of interest in this work.

628

629

630

631

632

633

634

635

636

# 8. Declaration of generative Al and Al-assisted technologies in the writing process

During the preparation of this work, we used DeepL Write and Al Studio (Google) in order to provide language refinement and proofreading purposes during the preparation of this manuscript. These tools were used to improve clarity and coherence without changing the scientific content or interpretations. All intellectual contributions and the final responsibility for the content remain solely with us. After using this tool/service, we reviewed and edited the content as needed and take full responsibility for the content of the publication.

637

638

639

640

### 9. References

- 1. Welsch ME, Snyder SA, Stockwell BR. Privileged scaffolds for library design and drug discovery. *Curr Opin Chem Biol.* 2010;14(3):347-361.
- 641 2. Kim J, Kim H, Park SB. Privileged Structures: Efficient Chemical "Navigators" toward 642 Unexplored Biologically Relevant Chemical Spaces. *J Am Chem Soc.* 2014;136(42):14629-643 14638.

- 644 3. Huang Z, Xie N, Illes P, et al. From purines to purinergic signalling: molecular functions
- and human diseases. Signal Transduct Target Ther. 2021;6(1):162.
- 646 4. Klabunde T, Hessler G. Drug Design Strategies for Targeting G-Protein-Coupled
- 647 Receptors. *ChemBioChem*. 2002;3(10):928-944.
- 5. Shryock JC, Travagli HC, Belardinelli L. Evaluation of N-0861, (+-)-N6-endonorbornan-2-
- 649 yl-9-methyladenine, as an A1 subtype-selective adenosine receptor antagonist in the guinea pig
- isolated heart. *J Pharmacol Exp Ther*. 1992;260(3):1292-1299.
- 651 6. Chaparro S, Dittrich HC, Tang WW. Rolofylline (KW-3902): a new adenosine A1-receptor
- antagonist for acute congestive heart failure. *Future Cardiol*. 2008;4(2):117-123.
- 653 7. Bruns RF, Fergus JH, Badger EW, et al. Binding of the A1-selective adenosine
- 654 antagonist 8-cyclopentyl-1,3-dipropylxanthine to rat brain membranes. Naunyn Schmiedebergs
- 655 Arch Pharmacol. 1987;335(1).
- 656 8. Chang LCW, Künzel JKVFD, Mulder-Krieger T, et al. 2,6,8-Trisubstituted 1-Deazapurines
- as Adenosine Receptor Antagonists. *J Med Chem.* 2007;50(4).
- 658 9. Lambertucci C, Marucci G, Dal Ben D, et al. New potent and selective A1 adenosine
- receptor antagonists as potential tools for the treatment of gastrointestinal diseases. Eur J Med
- 660 *Chem.* 2018;151:199-213.
- 10. Kalk P, Eggert B, Relle K, et al. The adenosine A1 receptor antagonist SLV320 reduces
- 662 myocardial fibrosis in rats with 5/6 nephrectomy without affecting blood pressure. *Br J Pharmacol*.
- 663 2007;151(7):1025-1032.
- 664 11. Lambertucci C, Marucci G, Catarzi D, et al. A 2A Adenosine Receptor Antagonists and
- their Potential in NeurologicalDisorders. *Curr Med Chem.* 2022;29(28):4780-4795.
- 666 12. Pineda de las Infantas y Villatoro MJ, Unciti-Broceta JD, Contreras-Montoya R, et al.
- 667 Amide-controlled, one-pot synthesis of tri-substituted purines generates structural diversity and
- analogues with trypanocidal activity. *Sci Rep.* 2015;5(1):9139.
- 669 13. Lorente-Macías Á, Benítez-Quesada M, Molina IJ, Unciti-Broceta A, Díaz-Mochón JJ,
- Pineda de las Infantas Villatoro MJ. 1 H and 13 C Assignments of 6-, 8-, 9- Substituted Purines.
- 671 Magn Reson Chem. 2018;56(9):852-859.

- 672 14. Lorente-Macías A, Díaz-Mochón JJ, Pineda MJ, Unciti-Broceta A. Design and Synthesis
- of 9-Dialkylamino-6-[(1H-1,2,3-Triazol-4-YI)Methoxy]-9H-Purines. *ChemRxiv*. Published online
- 674 February 1, 2021.
- 675 15. Lorente-Macías Á, Iañez I, Jiménez-López MC, et al. Synthesis and screening of 6-
- alkoxy purine analogs as cell type-selective apoptotic inducers in Jurkat cells. *Arch Pharm Weinh*.
- 677 2021;354:2100095.
- 678 16. Martinez-Peinado N, Lorente-Macías Á, García-Salguero A, et al. Novel Purine
- 679 Chemotypes with Activity against Plasmodium falciparum and Trypanosoma cruzi.
- 680 *Pharmaceuticals*. 2021;14(7):638.
- 681 17. Gomez LC, Lorente-Macias A, Villatoro MJP de las I y, Garzon-Ruiz A, Diaz-Mochon JJ.
- 682 Symmetric 4,6-Dialkyl/arylamino-5-nitropyrimidines: Theoretical Explanation of Why Aminolysis of
- 683 Alkoxy Groups Is Favoured over Chlorine Aminolysis in Nitro-Activated Pyrimidines. Published
- 684 online May 4, 2023.
- 685 18. Barnadas-Carceller B, Martinez-Peinado N, Gómez LC, et al. Identification of compounds
- with activity against Trypanosoma cruzi within a collection of synthetic nucleoside analogs. Front
- 687 Cell Infect Microbiol. 2023;12. Accessed March 2, 2023.
- 688 19. Asgharkhah E, Jazi MS, Asadi J, Jafari SM. Role of A1 adenosine receptor in survival of
- 689 human lung cancer. *Gene Rep.* 2022;28:101649.
- 690 20. Leone RD, Emens LA. Targeting adenosine for cancer immunotherapy. J Immunother
- 691 Cancer. 2018;6(1):57.
- 692 21. Cheng Y, Prusoff WH. Relationship between the inhibition constant (K1) and the
- 693 concentration of inhibitor which causes 50 per cent inhibition (I50) of an enzymatic reaction.
- 694 Biochem Pharmacol. 1973;22(23):3099-3108.
- 695 22. Leff P, Dougall IG. Further concerns over Cheng-Prusoff analysis. *Trends Pharmacol Sci.*
- 696 1993;14(4):110-112.
- 697 23. Morris GM, Huey R, Lindstrom W, et al. AutoDock4 and AutoDockTools4: Automated
- docking with selective receptor flexibility. J Comput Chem. 2009;30(16):2785-2791.

- 699 24. Hanwell MD, Curtis DE, Lonie DC, Vandermeersch T, Zurek E, Hutchison GR. Avogadro:
- an advanced semantic chemical editor, visualization, and analysis platform. *J Cheminformatics*.
- 701 2012;4(1):17.
- 702 25. Frisch MJ, Trucks G, Schlegel HB, et al. Gaussian 09 Revision A.1. Gaussian Inc.
- 703 Published online January 1, 2009.
- 704 26. Dolinsky TJ, Nielsen JE, McCammon JA, Baker NA. PDB2PQR: an automated pipeline
- 705 for the setup of Poisson-Boltzmann electrostatics calculations. Nucleic Acids Res. 2004;32(Web
- 706 Server):W665-W667.
- 707 27. Pettersen EF, Goddard TD, Huang CC, et al. UCSF Chimera? A visualization system for
- exploratory research and analysis. *J Comput Chem.* 2004;25:1605-1612.
- 709 28. Pelleg A, Hurt CM. Effects of N6-endonorbornan-2-yl-9-methyladenine, N0861, on
- 710 negative chronotropic and vasodilatory actions of adenosine in the canine heart in vivo. Can J
- 711 *Physiol Pharmacol.* 1992;70(11):1450-1456.
- 712 29. Pires DEV, Blundell TL, Ascher DB. pkCSM: Predicting Small-Molecule Pharmacokinetic
- and Toxicity Properties Using Graph-Based Signatures. *J Med Chem.* 2015;58(9):4066-4072.
- 714 30. Klotz KN, Hessling J, Hegler J, et al. Comparative pharmacology of human adenosine
- 715 receptor subtypes characterization of stably transfected receptors in CHO cells. Naunyn
- 716 Schmiedebergs Arch Pharmacol. 1997;357(1):1-9.
- 717 31. FREDHOLM BB, IJZERMAN AP, JACOBSON KA, KLOTZ KN, LINDEN J. International
- Union of Pharmacology. XXV. Nomenclature and Classification of Adenosine Receptors.
- 719 Pharmacol Rev. 2001;53(4):527-552.
- 720 32. Gao Z, Jacobson KA. 2-Chloro-N6-cyclopentyladenosine, adenosine A1 receptor agonist,
- antagonizes the adenosine A3 receptor. *Eur J Pharmacol*. 2002;443:39-42.
- 723 **Table 1** Binding affinity results for the four hAR (A<sub>1</sub>, A<sub>2A</sub>, A<sub>2B</sub> and A<sub>3</sub>) of the adenine derivatives
- 724 (see Fig. 1) and reference standards (XAC, CGS-15943, ZM241385, and MRS1220) presented in
- 725 the manuscript

## Receptors

Compounds	hA <sub>1</sub>		hA <sub>2A</sub>		hA <sub>2B</sub>			hA <sub>3</sub>	
•	% Inhib.	K <sub>i</sub> (nM)	% Inhib.	K <sub>i</sub> (nM)	% Inhib.	K <sub>i</sub> (nM)	% Inhib.	K <sub>i</sub> (nM)	
11a	43±1		8±3		32±4		45±4		
11b	41±1		4±2		44±3		35±1		
11c		458.8±13	33±4			1091.0±35	28±1		
12a	49±2		7±1		12±1		30±3		
12b	38±1		5±2		18±3		21±3		
12c		620.4±25	8±3		44±1		48±5		
13a	27±2		16±2		2±2		11±3		
13b	29±2		17±4		17±2		24±2		
13c		880.2±31	24±1		3±1		37±4		
14a	55±5		11±3		22±3		21±1		
14b	36±2		4±2		26±4		20±1		
14c		2.0±0.3	33±2		55±5			211.2±53	
15a	20±2		23±3		1±1		30±5		
15c		71.9±36.6	27±1		8±3		5±2		

16a	36±5		23±3		2±1		13±4	
16b	24±1		11±3		5±3		14±3	
16c	20±1		2±2		4±1		7±3	
17c		28±4		2664±42		1503±22		1482±34
18c		20±2	30±1			764±60		334±13
19c		46±10	42±2		57 ± 4		42±1	
XAC		13.9±2.2ª						
CGS-15943				1.4±0.3 <sup>b</sup>				
ZM 241385						28.3±4.4°		
MRS 1220								3.6±0.7 <sup>d</sup>

<sup>a</sup>  $K_i$  = 29.1 nM, reported by Klotz et al.<sup>30 b</sup>  $K_i$  = 4.3 nM, reported by Fredholm et al.<sup>31 c</sup>  $K_i$  = 32.0 nM, 727

reported by Fredholm et al.<sup>31</sup>.  $^{d}$  K<sub>i</sub> = 1.7 nM, reported by Gao & Jacobson.<sup>32</sup> n = 3. Note: 728

Compound 15b has been synthetized, but the yield has been very low. Therefore, and because 729

its substituents do not belong to the most active series, this molecule was no further evaluated.

731

732

733

730

Table 2. Antagonist potency (K<sub>B</sub>) against hA<sub>1</sub>AR of the adenine derivatives 11c, 12c, 14c, 15c,

17c, 18c and 19c and the reference standard XAC

734

735

ompound	R₁

Ř<sub>1</sub>

K<sub>B</sub> (nM)

*h*A₁AR

11c	Bn-	1272.2±268.5
12c	PhEt	550.7±232.6
14c	<sup>i</sup> Pr	24.9±19.4
15c	pClBn	687.2±32.7
17c	Et	50.7±9.45
18c	<sup>į</sup> Bu	83.6±28.2
19c	сР	99.7±10.4
XAC <sup>a</sup>		37.9±20.2

737

Table 3. Cell lines used for phenotypic screening of compounds 14c, 17c, 18c, and 19c.

738

Origin	Field of use
Primary colorectal adenocarcinomas	Colorectal cancer research
Colorectal carcinoma	Colorectal cancer research
Chronic myelogenous leukemia	
(CML)	Hematological research, leukemia,
Breast adenocarcinoma (triple-	
negative)	TNBC research (highly aggressive)
	Non-small cell lung cancer (NSCLC)
Human lung carcinoma	research
	Primary colorectal adenocarcinomas  Colorectal carcinoma  Chronic myelogenous leukemia  (CML)  Breast adenocarcinoma (triplenegative)

739

740

741

Table 4. EC<sub>50</sub> (µM) values of compounds as antiproliferative agents across various cancer cell

742 lines. n = 3

Compound SW480 SW48 HCT116 K562	MDA-MB-231 A549
---------------------------------	-----------------

14c	40 ± 12.14	79 ± 35.65	78 ± 37.99	35 ± 0.93	37 ± 11.33	62 ±
140	40 1 12.14	79 ± 33.03	10 ± 31.99	33 I 0.93	07 ± 11.00	33.56
17c	>100	>100	>100	>100	30 ± 0.61	77 ±
110		7 100	7 100	7 100	00 1 0.01	40.41
18c	13 ± 3.77	>100	>100	17 ± 8.82	53 ± 40.41	>100
19c	7 ± 0.71	10 ± 0.27	12 ± 2.63	13 ± 9.01	15 ± 5.06	39 ± 9.48

Abbreviations: AR: Adenosine Receptor; GPCR: G protein-coupled receptor; *h*A<sub>1</sub>AR: human adenosine A1 receptor; *h*A<sub>2</sub>AAR: human adenosine A2A receptor; *h*A<sub>2</sub>BAR: human adenosine A2B receptor; *h*A<sub>3</sub>AR: human adenosine A3 receptor; N-0861: N6-endonorbonan-2-yl-9-methyladenine; TLC: Thin-Layer Chromatography; NMR: Nuclear Magnetic Resonance; CDCl3: Deuterated Chloroform; ES: Electrospray Ionization; HPLC: High-Performance Liquid Chromatography; TEA: Triethylamine; DPCPX: 1,3-dipropyl-8-cyclopentylxanthine; NECA: 5'-(N-ethylcarboxamido)adenosine; R-PIA: R-Phenylisopropyladenosine; Tris-HCl: Tris(hydroxymethyl)aminomethane hydrochloride; EDTA: Ethylenediaminetetraacetic acid; cAMP: cyclic adenosine monophosphate; EIA: Enzyme Immunoassay; FSK: Forskolin; XAC: 8-Cyclopentyl-1,3-dipropylxanthine; DMSO: Dimethyl Sulfoxide; AD4: AutoDock 4 PDB: Protein Data Bank; RMSD: Root-Mean-Square Deviation; TSPA: Total Solvent-Accessible Surface Area cLogP: Calculated octanol-water partition coefficient; ADME: Absorption, Distribution, Metabolism, and Excretion; DMPK: Drug Metabolism and Pharmacokinetics; BBB: Blood-Brain Barrier; Fu: Fraction Unbound in Human Plasma; IC50: Half maximal inhibitory concentration; EC50: Half-maximal effective concentration; mRNA: messenger ribonucleic acid.

761 Scheme 1. Synthetic methodology. Reagents and conditions: a) Propargyl alcohol, DBU, THF, rt, 762 1 h; b) R1-NH<sub>2</sub>, TEA, DCM, rt, 30 min.; c) SnCl<sub>2</sub>2H<sub>2</sub>O, EtOH, reflux, 1 h, d) (CH<sub>3</sub>)<sub>3</sub>CR<sup>2</sup>, CH<sub>3</sub>SO<sub>3</sub>H, 110 °C, 24 h. cP = cyclopentyl. The synthesis of compounds 11-15 (a-c) and their intermediates 763 764 is described elsewhere.<sup>18</sup> 765 766 Figure 1. The first series of adenine 11-16(a-c) derivatives tested to measure their binding affinity to human adenosine receptors. R<sup>2</sup> = H (family a), methyl (family b), and phenyl (family c). 18 767 768 769 Figure 2. Bisalkyl compounds synthesized based on 14c as the lead structure and the well-770 known hA1AR inhibitors N-0861 and N-cyclopentyl-9-methyl-8-phenyl-adenine. 771 772 Figure 3. A) scatter plot showing the correlation between median-of-ratio normalized ADORA1 773 mRNA expression and the log-transformed half-maximal inhibitory concentration (EC<sub>50</sub>) of **19c** 774 across various cancer cell lines. The Pearson correlation coefficient (R = -0.57) indicates a negative correlation, but it is not statistically significant (p = 0.24). The blue line represents the 775 776 linear regression, and the grey shaded area represents the 95% confidence interval. B) Boxplot 777 separating cell lines based on their median ADORA1 expression, with a left cutoff of 217 and a 778 right cutoff of 131. The corresponding log-transformed half-maximal inhibitory concentration  $(EC_{50})$  of **19c** is also shown. 779 780 781 Figure 4. (a) Predicted binding pose of 14c (blue) on hA1AR (PDB ID: 5UEN, tan); (b) 782 Superposition of the active conformation of hA1AR (PDB ID: 7LD4, dark gray) with the natural 783 agonist adenosine (orange) and the predicted binding pose of 14c (blue) on hA1AR (PDB ID: 784 5UEN, tan); (c) superimposition of the covalently bound hA1AR-selective antagonist DU172 (pink) 785 and the predicted binding pose of 14c (blue) on the inactive conformation of hA1AR (PDB ID: 5UEN, tan); (d) Surface superposition of active (PDB ID: 7LD4, dark gray) and inactive (PDB ID: 786 5UEN, tan) conformations of  $hA_1AR$  with the predicted binding pose of **14c** (blue) and the natural 787

agonist adenosine (orange); (e) Predicted binding poses of 14c (blue) and 19c (red) on hA₁AR

(PDB ID: 5UEN, tan); (f) Surface superposition of active (PDB ID: 7LD4, dark gray) and inactive (PDB ID: 5UEN, tan) conformations of  $hA_1AR$  with the predicted binding pose of **14c** (blue) and **19c** (red). Hydrogen bonds are shown as dashed yellow lines. **Figure 5.** (a) Superposition of  $hA_1AR$  (PDB ID: 5UEN, tan) and  $hA_{2A}AR$  (PDB ID: 4EIY, purple) with predicted binding pose of **19c** (dark green) and **14c** (light green) on  $hA_{2A}AR$ ; (b) surface representation of the inactive conformation of  $hA_{2A}AR$  (PDB ID: 4EIY, purple) and  $hA_1AR$  (PDB ID: 5UEN, tan) with predicted binding poses of **19c** (dark green) and **14c** (light green). Hydrogen bonds are represented by dashed yellow lines.

## 799 **Scheme 1.**

CI NO<sub>2</sub> NHR<sup>1</sup> NHR<sup>1</sup> NHR<sup>1</sup> 
$$\frac{1}{C}$$
 NHR<sup>1</sup>  $\frac{1}{C}$  NHR<sup>2</sup>  $\frac{1}{C}$ 

**2**: R<sup>1</sup>= Bn 55% **11**: R<sup>1</sup>= Bn 77% **12**: R<sup>1</sup>= PhEt 78%

4:  $R^1$ = pCH3OBn 72%13:  $R^1$ = pCH3OBn 33%Family a:  $R^2$ = H5:  $R^1$ = P 92%14:  $R^1$ = P 33%Family b:  $R^2$ = Me6:  $R^1$ = pCIBn 95%15:  $R^1$ = pCIBn 77%Family c:  $R^2$ = Ph

7: R<sup>1</sup>= <sup>t</sup>Bu (not isolated)

8: R<sup>1</sup>= Et 84 %

9: R<sup>1</sup>= <sup>i</sup>Bu 83%

10: R<sup>1</sup>= cP 76%

16: R<sup>1</sup>= <sup>i</sup>Bu 43%

17: R<sup>1</sup>= Et 32%

18: R<sup>1</sup>= <sup>i</sup>Bu 59%

19: R<sup>1</sup>= cP 45%

800

801

### Aromatic substituents

### Non-aromatic substituents

804

805

## Figure 2

## N-cyclopentyl-9-methyl-8-phenyl-adenine

N-0861

## **Figure 3**

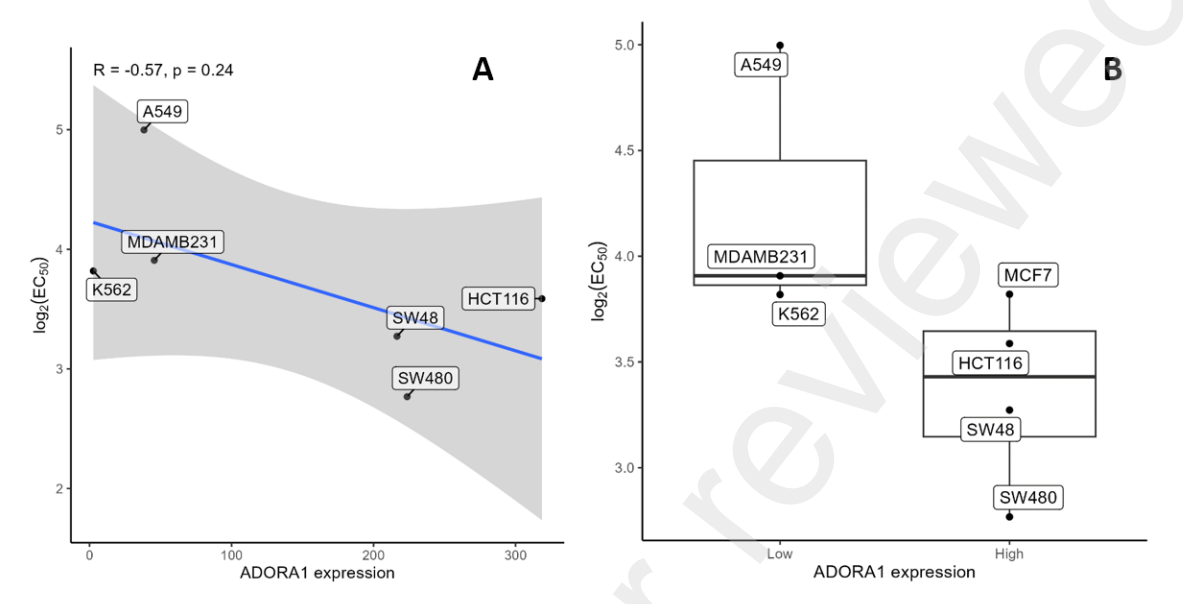
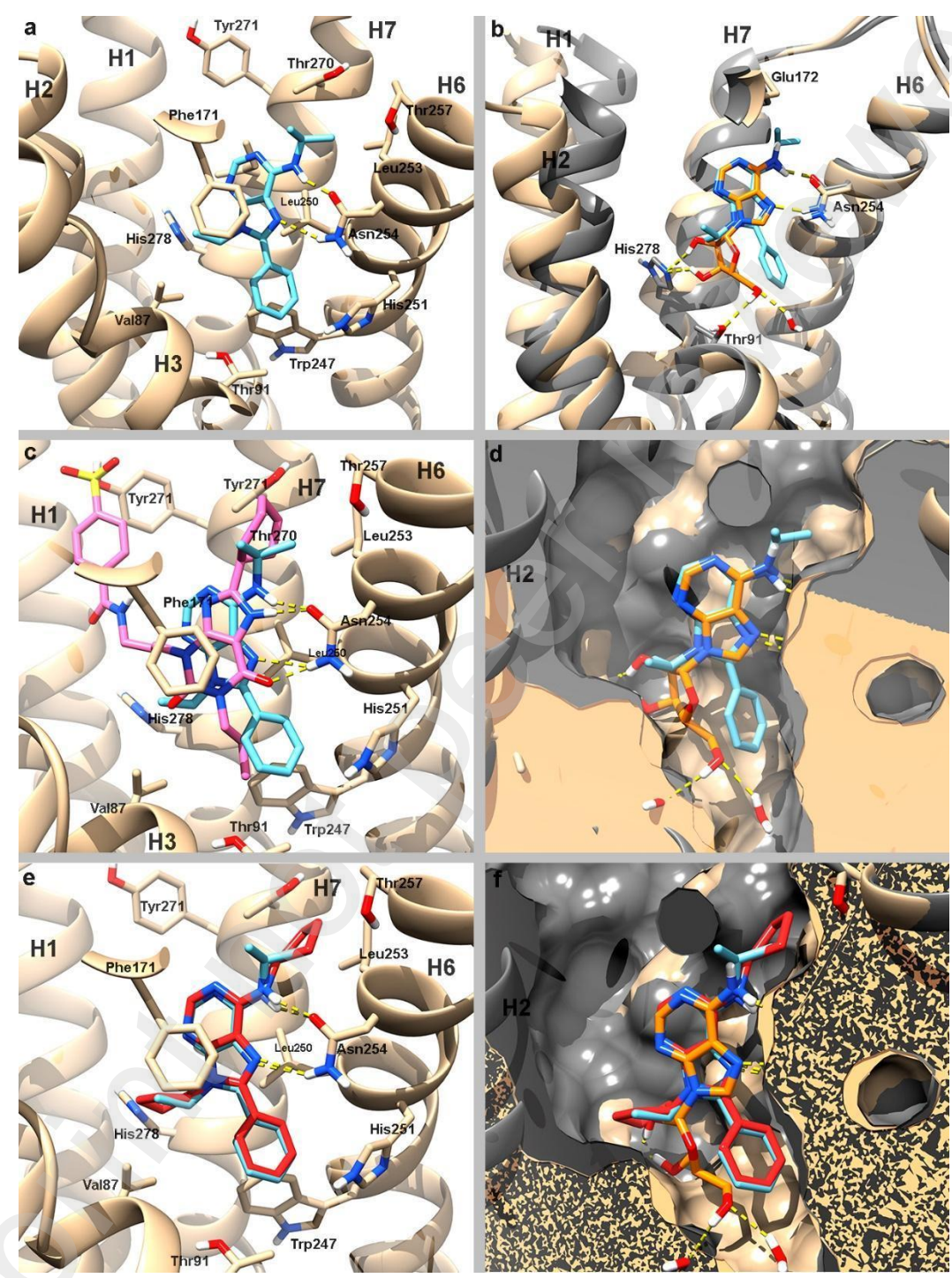


### Figure 4

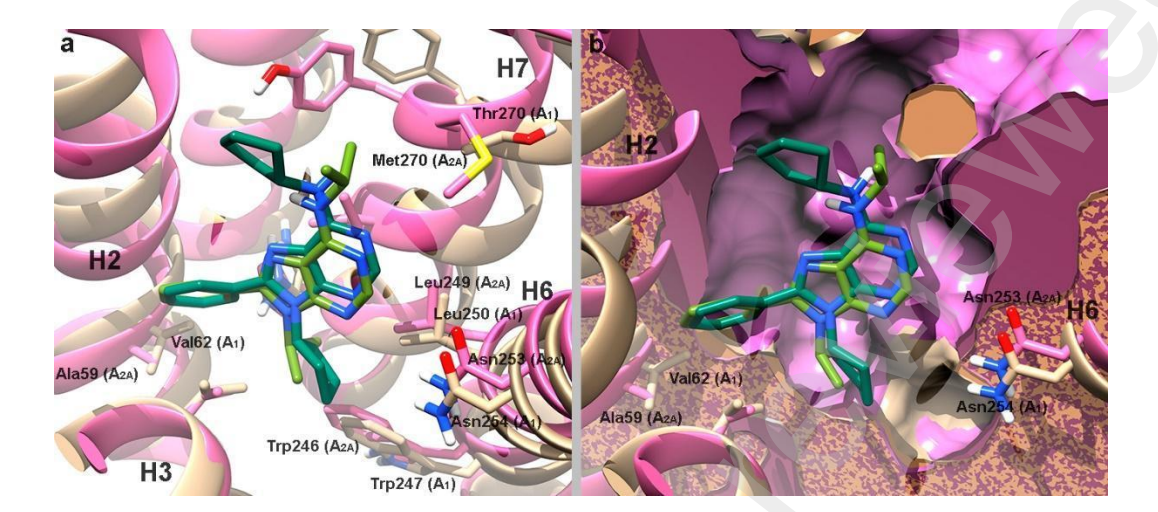


38

814

815

# **Figure 5**



CI NHR<sup>1</sup> NHR<sup>1</sup> NHR<sup>1</sup> 
$$R^1$$
 NHR<sup>1</sup>  $R^1$  NHR<sup>1</sup>  $R^2$   $R^2$   $R^1$   $R^2$   $R^$ 

4: 
$$R^1$$
=  $pCH_3OBn$ 

**7**: 
$$R^1 = {}^tBu$$

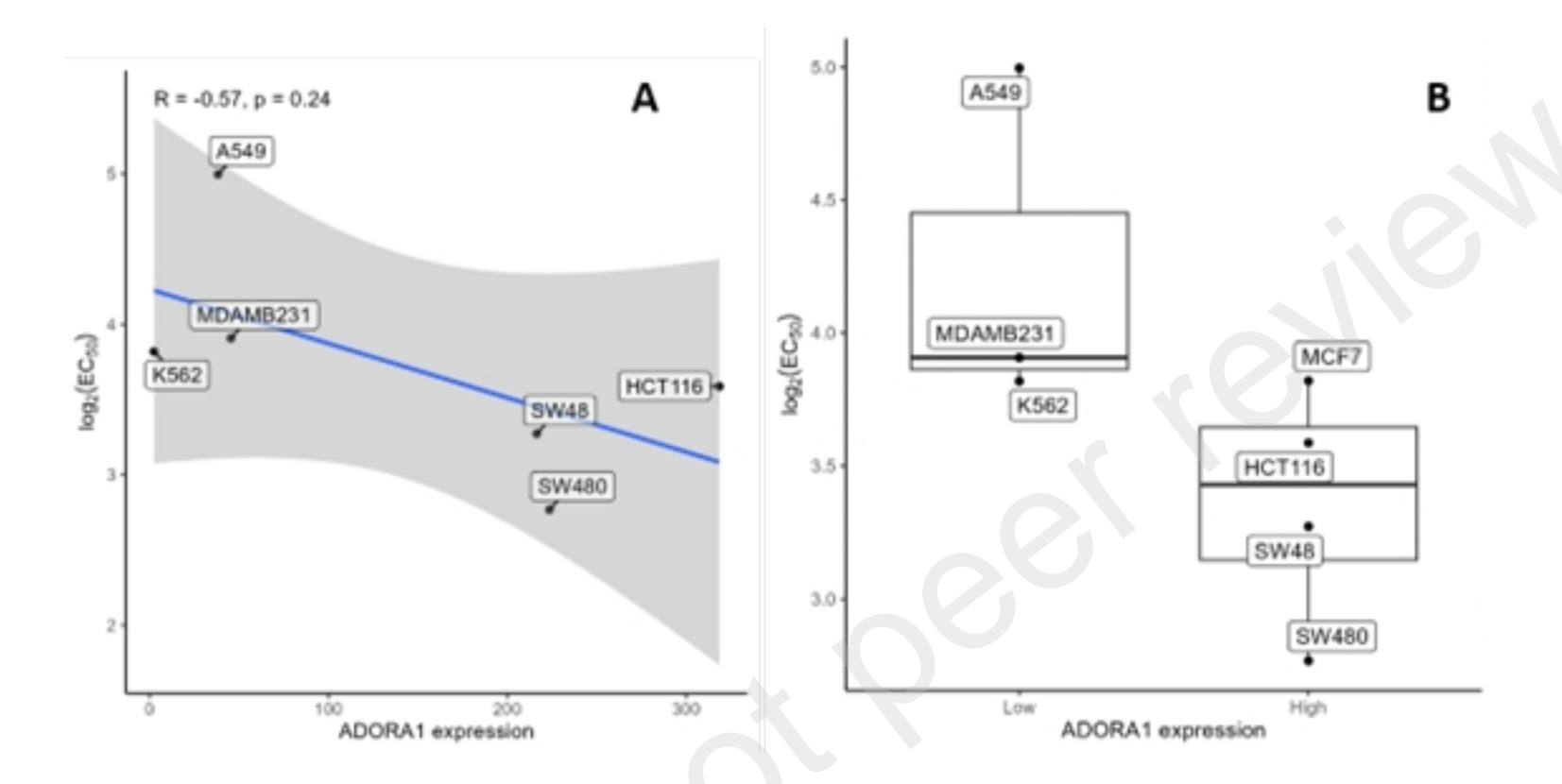
Family a:  $R^2$ = H

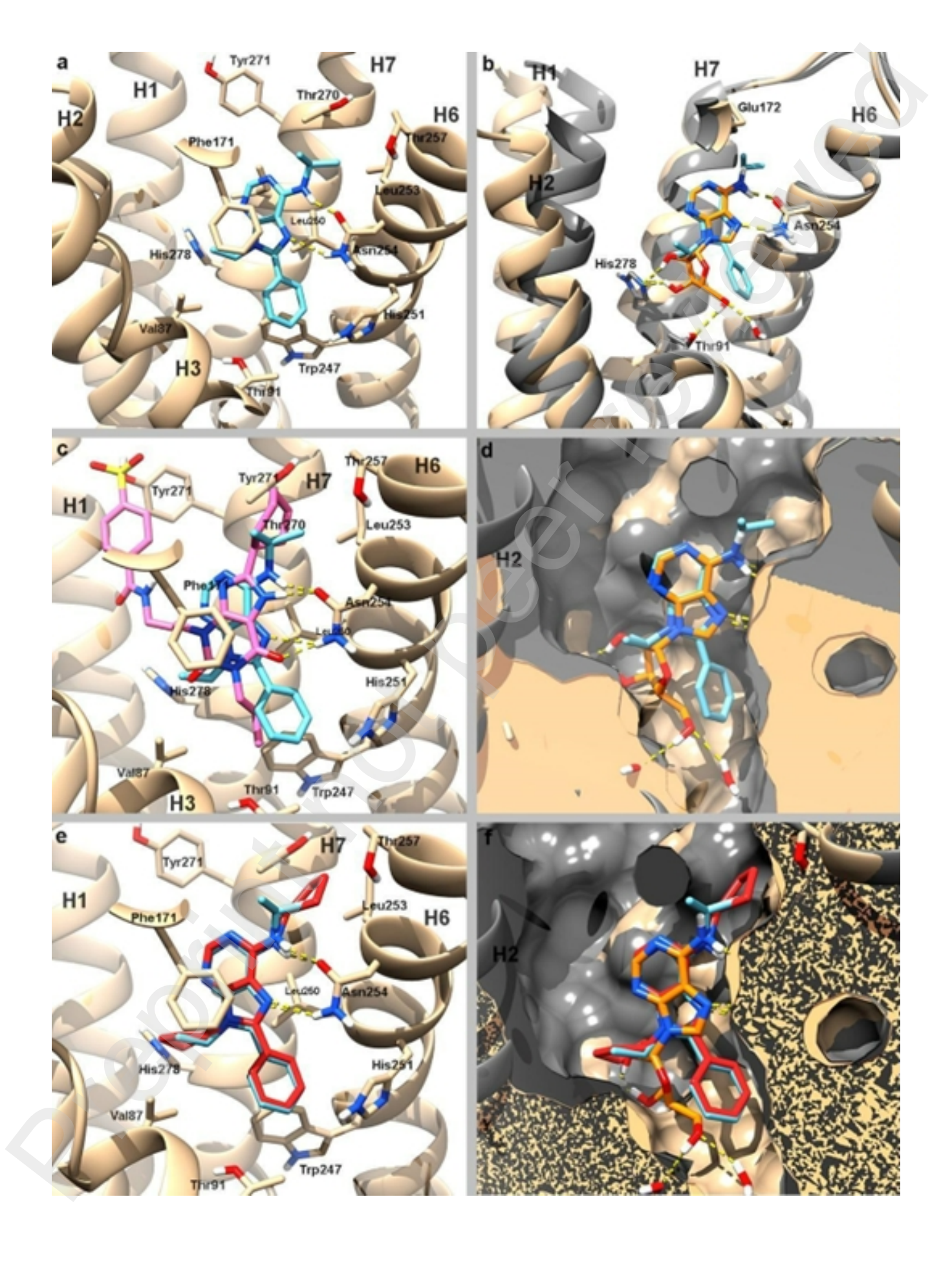
Family b: R<sup>2</sup>= Me

Family c:  $R^2$  = Ph

17c

18c





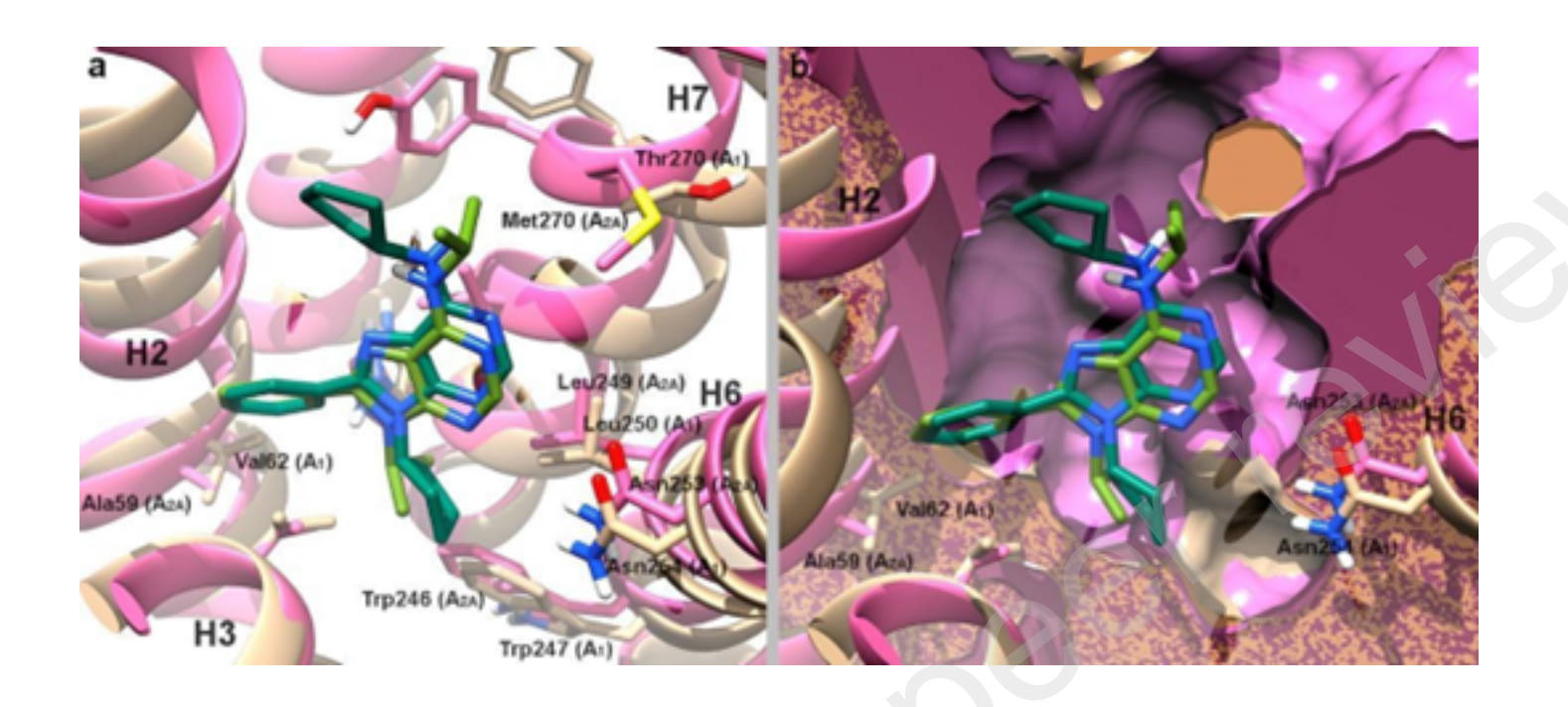


**Table 1** Binding affinity results for the four hAR (A<sub>1</sub>, A<sub>2A</sub>, A<sub>2B</sub> and A<sub>3</sub>) of the adenine derivatives (see Fig. 1) and reference standards (XAC, CGS-15943, ZM241385, and MRS1220) presented in the manuscript

### Receptors

Compounds	hA₁		hA <sub>2A</sub>		hA <sub>2B</sub>		hA <sub>3</sub>	
Composition	% Inhib.	K <sub>i</sub> (nM)	% Inhib.	K <sub>i</sub> (nM)	% Inhib.	K <sub>i</sub> (nM)	% Inhib.	K <sub>i</sub> (nM)
11a	43±1		8±3		32±4		45±4	
11b	41±1		4±2		44±3		35±1	
11c		458.8±13	33±4			1091.0±35	28±1	
12a	49±2		7±1		12±1		30±3	
12b	38±1		5±2		18±3		21±3	
12c		620.4±25	8±3		44±1		48±5	
13a	27±2		16±2		2±2		11±3	
13b	29±2		17±4		17±2		24±2	
13c		880.2±31	24±1		3±1		37±4	
14a	55±5		11±3		22±3		21±1	
14b	36±2		4±2		26±4		20±1	
14c		2.0±0.3	33±2		55±5			211.2±53
15a	20±2		23±3		1±1		30±5	

15c		71.9±36.6	27±1		8±3		5±2	
16a	36±5		23±3		2±1		13±4	
16b	24±1		11±3		5±3		14±3	
16c	20±1		2±2		4±1		7±3	
17c		28±4		2664±42		1503±22		1482±34
18c		20±2	30±1			764±60		334±13
19c		46±10	42±2		57 ± 4		42±1	
XAC		13.9±2.2ª						
CGS-15943				1.4±0.3b				
ZM 241385						28.3±4.4°		
MRS 1220								3.6±0.7 <sup>d</sup>

<sup>&</sup>lt;sup>a</sup>  $K_i$  = 29.1 nM, reported by Klotz et al.<sup>30 b</sup>  $K_i$  = 4.3 nM, reported by Fredholm et al.<sup>31 c</sup>  $K_i$  = 32.0 nM, reported by Fredholm et al.<sup>31</sup> d  $K_i$  = 1.7 nM, reported by Gao & Jacobson.<sup>32</sup> n = 3. Note: Compound **15b** has been synthetized, but the yield has been very low. Therefore, and because its substituents do not belong to the most active series, this molecule was no further evaluated.

Table 2. Antagonist potency (K<sub>B</sub>) against hA<sub>1</sub>AR of the adenine derivatives 11c, 12c, 14c, 15c,

### 17c, 18c and 19c and the reference standard XAC

R <sub>1</sub> NH N N N N N N N N N N N N N N N N N N		
		<i>h</i> A₁AR
Compound	R <sub>1</sub>	K <sub>B</sub> (nM)
11c	Bn-	1272.2±268.5
12c	PhEt	550.7±232.6
14c	<sup>i</sup> Pr	24.9±19.4
15c	pClBn	687.2±32.7
17c	Et	50.7±9.45
18c	<sup>i</sup> Bu	83.6±28.2
19c	сР	99.7±10.4
XACª		37.9±20.2

Table 3. Cell lines used for phenotypic screening of compounds 14c, 17c, 18c, and 19c.

Cell Line	Origin	Field of use
SW480, SW48	Primary colorectal adenocarcinomas	Colorectal cancer research
HCT116	Colorectal carcinoma	Colorectal cancer research
	Chronic myelogenous leukemia	
K562	(CML)	Hematological research, leukemia,
	Breast adenocarcinoma (triple-	
MDA-MB-231	negative)	TNBC research (highly aggressive)
		Non-small cell lung cancer (NSCLC)
A549	Human lung carcinoma	research

**Table 4.** EC<sub>50</sub> ( $\mu$ M) values of compounds as antiproliferative agents across various cancer cell lines. n = 3

Compound	SW480	SW48	HCT116	K562	MDA-MB-231	A549
14c	40 ± 12.14	79 ± 35.65	78 ± 37.99	35 ± 0.93	37 ± 11.33	62 ± 33.56
17c	>100	>100	>100	>100	30 ± 0.61	77 ± 40.41
18c	13 ± 3.77	>100	>100	17 ± 8.82	53 ± 40.41	>100
19c	7 ± 0.71	10 ± 0.27	12 ± 2.63	13 ± 9.01	15 ± 5.06	39 ± 9.48